J Solid State Electrochem (2012) 16:2883–2889
DOI 10.1007/s10008-012-1720-9

ORIGINAL PAPER

Preparation of electrochemically reduced graphene oxide-modified electrode and its application for determination of *p*-aminophenol

Su-juan Li · De-Hua Deng · Huan Pang · Lin Liu · Yun Xing · Shui-Ren Liu

Received: 28 December 2011 / Revised: 3 March 2012 / Accepted: 7 March 2012 / Published online: 20 March 2012

Abstract A simple and eco-friendly electrochemical method to reduce graphene oxide precursor was employed for fabrication of graphene sheets modified glassy carbon electrode, and then, the resulting electrode [electrochemically reduced graphene oxide (ERGO)/glassy carbon electrode (GCE)] was used to determine *p*-aminophenol. The experimental results demonstrated that the modified electrode exhibited excellent electrocatalytic activity toward the redox of *p*-aminophenol as evidenced by the significant enhancement of redox peak currents and the decreased peak-to-peak separation in comparison with a bare GCE. A highly sensitive and selective voltammetry determination of *p*-aminophenol is developed using the ERGO/GCE. This method has been applied for the direct determination of *p*-aminophenol in artificial wastewater.

Keywords Electrochemically reduced graphene oxide · Modified electrode · *p*-Aminophenol · Voltammetry

Introduction

p-Aminophenol (*p*-AP) is a synthetic intermediate or a degradation product of the antipyretic and analgesic drug paracetamol, and has been found to be detected in pharmaceutical preparation of paracetamol [1]. Because of the distinct nephrotoxicity and teratogenic effect of *p*-AP, the maximum content of *p*-AP in pharmaceuticals has been limited to 50 ppm by the United States and European pharmacopeia [2]. In addition, *p*-AP is used as a fundamental chemical material for the production of chemical inhibitor, dyestuff, developer, and so on, which result in a substantive release of *p*-AP into the environment as ecological pollutants. So far, the content of *p*-AP in discharged wastewater should be less than 1.0 mg L^{-1} according to the standard of China [3]. Therefore, in view of major concerns about health and environmental protection, it is necessary to develop a simple, fast, sensitive, and accurate analytical method for determining *p*-AP in pharmaceutical tablets and wastewater.

At present, a number of methods have been proposed to determine *p*-AP, such as chromatography [4], capillary electrophoresis [5], spectrophotometry [6], and electrochemical methods [7, 8]. Among these methods, the former three techniques usually require a complicated sample pretreatment process, expensive instruments, and long analysis time that make them unsuitable for routine analysis. Since *p*-AP is electroactive, and most electroanalytical techniques are less time-consuming, inexpensive, selective, highly sensitive, have good reliability and quick response, electrochemical techniques can be considered as a strong alternative to the abovementioned methods for the determination of *p*-AP. The electrochemical detection of *p*-AP at the conventional electrode by voltammetry is difficult owing to the high overpotential and poor sensitivity. Recently, much effort has been made to developing nanomaterial-modified electrodes for the purpose of achieving sensitive and selective determination of *p*-AP.

Graphene, a single layer of carbon atoms packed into a dense honeycomb crystal structure, was a novel and promising carbon material since experimentally discovered in 2004 due to its unique nanostructure and extraordinary properties [9–11]. Graphene sheets have high electrocatalytic activities and extraordinary electronic transport properties, and they have been investigated as

S.-j. Li (✉) · D.-H. Deng · H. Pang · L. Liu · Y. Xing · S.-R. Liu
School of Chemistry and Chemical Engineering,
Anyang Normal University,
Anyang 455002, China
e-mail: lisujuan1981@gmail.com

electrode modifications in fields of electrochemistry and electroanalytical chemistry [12, 13]. For instance, it has been reported that graphene film-based biosensors have the capability for simultaneous determination of biomolecules such as dopamine, ascorbic acid, and uric acid [14]. Nafion/graphene nanocomposite films were utilized as enhanced sensing platform for ultrasensitive determination of lead and cadmium [15, 16]. Also, Lin's group has utilized the graphene-modified electrodes to obtain a high-performance electrochemical sensor for paracetamol [17]. However, graphene films on electrodes in these researches are usually prepared by chemical reduction of graphene oxide (CRGO) sheets [18–20]. Such a preparation methodology involves some toxic chemicals. Recently, electrochemical reduction of graphene oxide (GO) to graphene, which has been reported by several research groups [21–23], has arisen more interest due to its fast and green nature. Generally, GO is first assembled on the electrodes as precursor by solution deposition methods, and then is subjected to electrochemical reduction. Here, by using electrons as the reducing agent, this method is green, fast, simple, and will not result in contamination of the synthesized material. In addition, the as-prepared electrochemically reduced GO, named as ERGO, are directly immobilized on the conducting substrate (electrode), facilitating widespread applications in chemical sensors and biosensors [24, 25]. Furthermore, this method was further expanded to achieve one-step electrochemical synthesis of graphene-based nanocomposites, such as graphene/metal nanoparticles [26], graphene/metal oxides [27], graphene/conducting polymers [28], and so on. Therefore, the electrochemical performances and applications of electrochemically reduced graphene oxide are promising and will be further developed.

In this paper, a simple, economical, and eco-friendly method was used to fabricate ERGO-modified glassy carbon electrode by applying a constant cathodic potential on GO/glassy carbon electrode (GCE), and a new electrochemical sensor for sensitive and selective determination of *p*-AP using the ERGO-modified electrode was presented. Compared with the bare glassy carbon electrode, ERGO-modified electrode could intensively enhance the redox peak currents and decrease the overpotentials of *p*-AP. In addition, the oxidation peak currents of *p*-AP were found to be sensitively responding to the *p*-AP concentration, and a good percentage of recoveries was obtained at the modified electrode when it was used to determine *p*-AP in real water samples. Based on these results, we believe it is a promising method for on-site analysis of *p*-AP in wastewater and practical industrial product. This work would enlarge the application range of graphene in electroanalytical chemistry.

Experimental

Apparatus

Electrochemical measurements were performed on a CHI 832 electrochemical workstation (Shanghai Chenhua Instrument Company, China). A conventional three-electrode system was used throughout the experiments. The working electrode was a GCE (d=3 mm), graphene oxide-modified GCE (GO/GCE), or electrochemically reduced graphene oxide-modified GCE (ERGO/GCE); the Ag/AgCl (3 mol L^{-1} KCl) electrode was the reference electrode and a platinum wire as the auxiliary electrode. The ultrasonic cleaner (KQ 100E, 100 W, Kunshan, China) was used to exfoliate GO. The morphology of synthesized ERGO sheets was characterized using scanning electron microscopy (SEM, Hitachi, S-4800, 15 kV). All the pH values were measured with a PHS-3C precision pH meter (Leici Devices Factory of Shanghai, China), which was calibrated with standard buffer solutions every day.

Reagents and solutions

p-AP (obtained from Aladdin Reagent Co. Ltd, Shanghai, China) was used without further purification. Its stock solution was prepared with anhydrous ethanol and then stored at a refrigerator with 4 °C to avoid light. Phosphate buffer solution (PBS) was prepared by mixing the stock solutions of 0.1 M KH_2PO_4 and 0.1 M Na_2HPO_4 at different rations to adjust the pH value of 6.47. Spectral graphite (about 50 μm, Shanghai Carbon Co., Ltd.) was used to synthesize GO. Other chemicals were all of analytical grade. All experiments were carried out in a supporting electrolyte of PBS (0.1 M, pH 6.47) at room temperature (25±1 °C). Cyclic voltammetric experiments were performed with a scan rate of 100 mV s^{-1} unless otherwise stated.

Preparation of ERGO-modified electrode

Firstly, GO was synthesized from graphite by the modified Hummers method [29, 30]. The as-synthesized GO was suspended in water to give a brown dispersion, which was subjected to dialysis for 1 week to completely remove residual salts and acids. Exfoliated GO was obtained by ultrasound of the 0.5 wt% GO dispersion.

Prior to modification, the substrate GCE was polished successively with 0.3 and 0.05 μm Al_2O_3 power and rinsed thoroughly with doubly distilled water between each polishing step. After that, the GCE was sonicated in acetone and doubly distilled water each for 5 min, and dried under N_2 blowing. Then, 6 μL of the exfoliated GO dispersion was dispersed on the surface of pretreated GCE. After drying in air, a GO/GCE was obtained. Subsequently, the GO/GCE was immersed into 20 mM KH_2PO_4 solution, and a cathodic

potential of −0.7 V was applied to the GO/GCE by using potentiostat for about 10 min. By this method, ERGO/GCE was prepared. Then, it can be used for electrochemical analysis of *p*-AP.

Experimental procedure for electrochemical analysis

A certain volume of stock solution of *p*-AP and 10 mL 0.1 M PBS were added into an electrochemical cell, and then the three-electrode system was inserted into the cell. The cyclic voltammetry was performed at a scan rate of 100 mV s^{-1} to investigate the electrochemical behavior of the ERGO/GCE in analyte of *p*-AP. The differential pulse voltammogram (DPV) was recorded to achieve the quantitative analysis (with a step increment of 4 mV, pulse amplitude of 50 mV, and pulse period of 0.2 s).

Results and discussion

Characterization of ERGO-modified electrode

After GO sheets were deposited on the surface of glassy carbon electrode, referred to as GO/GCE, they were reduced by the electrochemical method, and ERGO sheets were obtained. Figure 1 shows the typical cyclic voltammograms (CVs) of GO electrolysis on GCE by scanning the potential from 0 to −1.5 V, where a large reduction current starting at about −0.6 V is observed during the first cycle of scanning. The large reduction current could be attributed to the reduction of the functional oxygen-containing groups on GO sheets [22]. Interestingly, in the following scanning cycles, the reduction peak disappears completely, which indicated that the electrochemical reduction of GO is irreversible. Based on these results, it is reasonable to speculate that GO can be effectively reduced when a cathodic potential more negative than −0.6 V is imposed. As observed from the inset of Fig. 1, slices of crumpled silk veil waves that were wrinkled and scrolled are obtained under a reduction potential of −0.7 V. This morphology is consistent with the reported results of graphene in literature [31–33]. The section of wrinkled structure is attributed to the π–π interaction within sheets of graphene. It is just this wrinkled nature that renders the graphene sheets stable and beneficial for maintaining a high surface area on the electrode.

Fourier transform infrared spectroscopy (FTIR) of the prepared ERGO films were also characterized (Fig. 2). Curve a shows the pure GO, the bands around 976, 1,056, 1,226, 1,276, 1,384, 1,580, and 1,727 cm^{-1} are attributed to the oxygen-containing functional groups on GO [21, 34], while the band at ca. 1,619 cm^{-1} could be due to the O–H stretching deformation vibration of intercalated water. After electrochemical reduction, the FTIR adsorption bands of oxygen functionalities decrease significantly and even disappear (curve b), which confirmed the successful conversion of GO into graphene.

Electrochemical behavior of *p*-AP at ERGO-modified electrode

The electrochemical behavior of *p*-AP on ERGO/GCE was investigated by CV. For comparison, the CVs of bare GCE and GO/GCE were also conducted. At the bare GCE (Fig. 3, curve a), a pair of relatively weak redox peak currents corresponding to the electrochemical redox of *p*-AP was observed at an anodic peak potential (E_{pa}) of 0.188 V and a cathodic peak potential (E_{pc}) of 0.112 V. When the GO films are deposited on GCE surface (Fig. 3, curve b), the redox peak currents of *p*-AP on GO/GCE both decrease obviously arising from the poor electrical conductivity of the deposited GO films. However, after electrochemical reduction, as can be seen from curve c of Fig. 3, *p*-AP exhibits a pair of well-defined redox waves on the ERGO/GCE with E_{pa}=0.145 V and E_{pc}=0.115 V, and the peak-to-peak separation (ΔE_p) is only 30 mV, indicating that fast electron transfer rate kinetics occur on ERGO/GCE. Compared

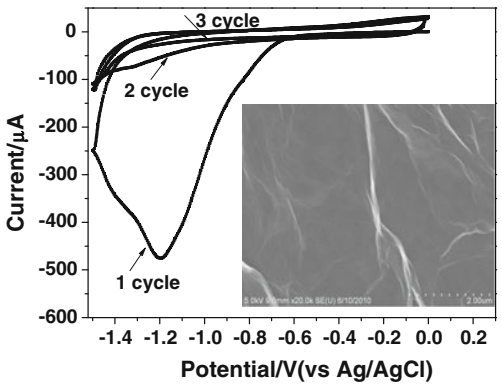

Fig. 1 CVs of GO/GCE in 20 mM KH_2PO_4. The *inset* was the SEM image of ERGO/GCE prepared at a cathodic potential of −0.7 V

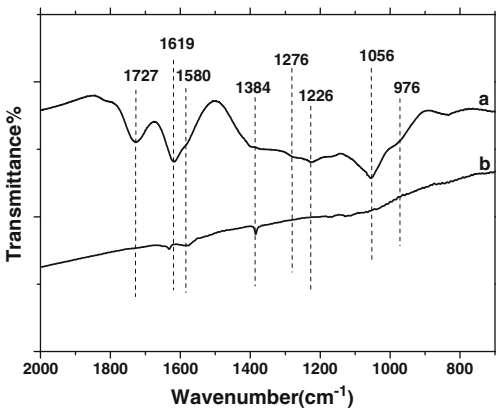

Fig. 2 FTIR spectra of GO (*a*) and ERGO films (*b*)

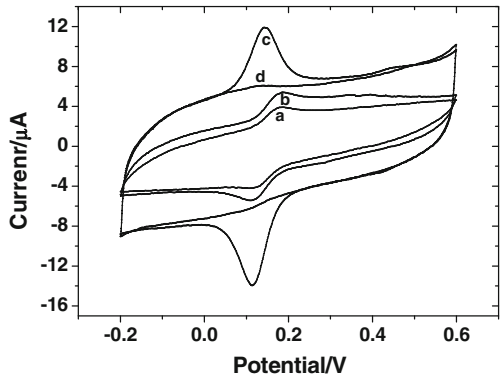

Fig. 3 CVs obtained for 0.1 mM *p*-AP at the bare GCE (*a*), GO/GCE (*b*), and ERGO/GCE (*c*) in 0.1 M PBS (pH 6.47) at a scan rate of 100 mV s^{-1}. *Curve d* is the CV of ERGO/GCE in the absence of *p*-AP

with the bare GCE or GO/GCE, the redox peak currents obtained on ERGO/GCE were much larger and the ΔE_p was much lower, which are clear evidences of excellent electrocatalytic activity of ERGO toward *p*-AP. In addition, the ΔE_p of *p*-AP on ERGO/GCE in this work is much smaller than that of 58 mV on CRGO-Chitosan/GCE [35], 114 mV on conductive polymer modified carbon fiber microelectrode (CFME) [8]. The electrochemistry of ERGO/GCE in pH 6.47 PBS was performed as control experiment (curve d), and no obvious redox currents were observed. Besides, it can also be seen from Fig. 3 that the background current of ERGO/GCE is much larger than that of the bare GCE, indicating high specific capacitance of graphene films on electrode.

Effect of electrochemical reduction potential on electroactivities of ERGO

ERGO prepared at different electrochemical reduction potentials will have different electrocatalytic activities toward *p*-AP. Figure 4 shows the CVs of ERGO/GCE fabricated at different cathodic potentials in 0.1 M PBS containing 0.1 mM *p*-AP at a scan rate of 100 mV s^{-1}. Obviously, with the negative shift of reduction potentials applied on GO/GCE, both the background currents and the redox peak currents of *p*-AP on the resulting ERGO/GCE increase significantly, indicating an enhanced electrical conductivity of ERGO films. However, when the potential is negative than −0.7 V, it is found that a new pair of redox peaks at 0.31/0.27 V appeared. The new redox peaks probably resulted from adsorption of *p*-AP at ERGO surface through π–π interactions. The more negative the applied potentials, the higher the delocalized electron density of ERGO, thus, the adsorption is stronger. To ensure enough detection

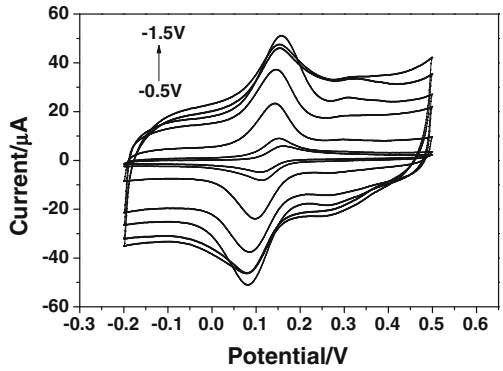

Fig. 4 CVs of ERGO/GCE prepared at different cathodic potentials of −0.5, −0.6, −0.7, −0.8, −0.9, −1.2, and −1.5 V in 0.1 mmol L^{-1} *p*-AP; the other conditions are the same as Fig. 3

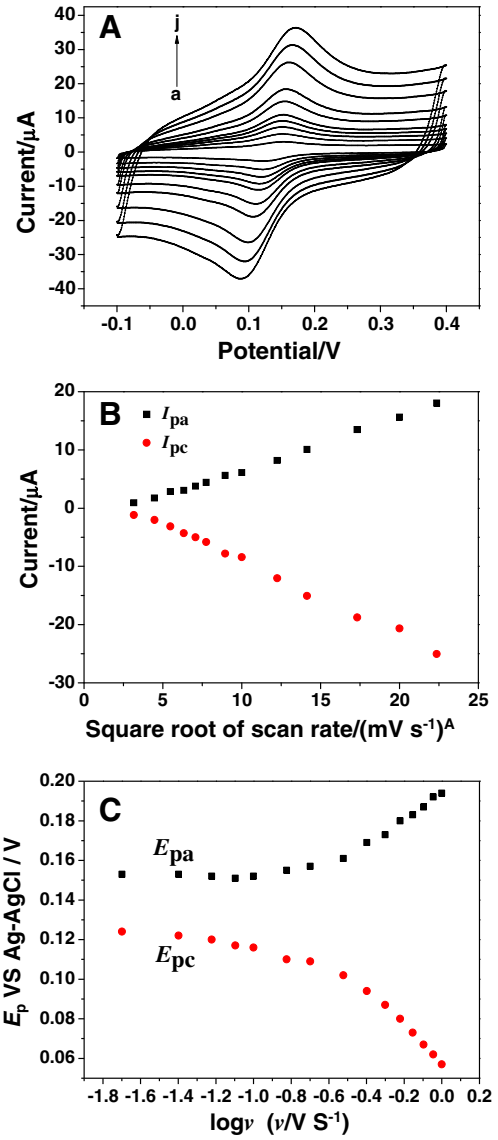

Fig. 5 **a** CVs acquired on ERGO/GCE with 0.1 mM *p*-AP in supporting electrolyte of 0.1 M PBS (pH 6.47) at different scan rates from 0.02, 0.04, 0.06, 0.08, 0.1, 0.15, 0.2, 0.3, 0.4, 0.5 V s^{-1} (from *a* to *j*). **b** The plot of the redox peak currents of *p*-AP versus scan rate. **c** The relationship between E_p and log *v*

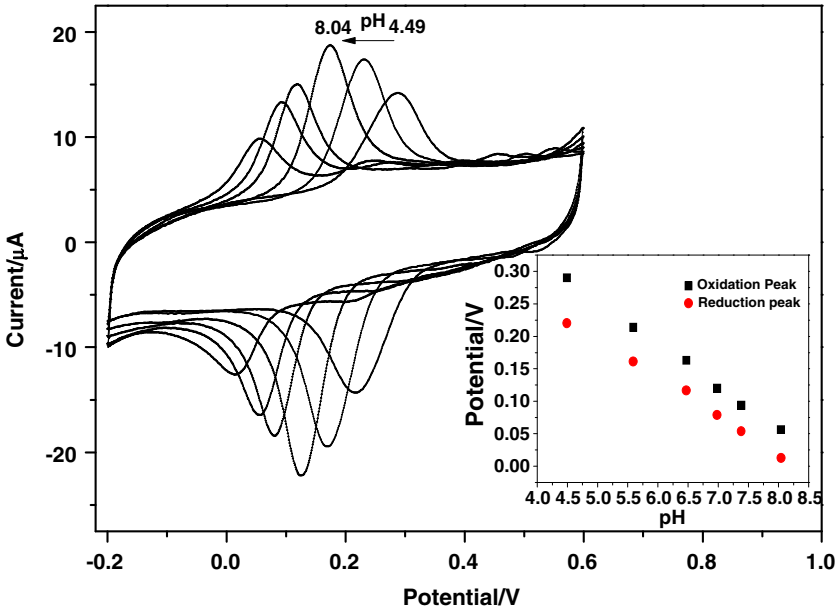

Fig. 6 CVs obtained at ERGO/GCE with 0.1 mM *p*-AP in the PBS with pH values of 4.49, 5.59, 6.47, 6.98, 7.38, and 8.04. *Inset* shows the plot of redox potentials versus pH values. Scan rate, 100 mV s^{-1}

sensitivity and relieve the fouling of electrode surface, a reduction potential of −0.7 V was selected to fabricate ERGO-modified electrode.

Effect of scan rate on the peak current and peak potential

To further investigate the mechanism of electrochemical redox of p-AP, the effect of scan rates (v) on the voltammetric response of *p*-AP on ERGO/GCE was investigated (Fig. 5a). It is clear that both the redox peak currents enhanced with increasing the potential scan rate. As can be seen in Fig. 5b, the redox peak currents were found linearly proportional to the square root of scan rate ranging from 0.02 to 0.5 Vs^{-1}. The linear regression equations are I_{pa} (microamps)=0.9021 $v^{1/2}$−2.4361 (v, millivolts per second, R=0.9966) and I_{pc} (microamps)= −1.2628 $v^{1/2}$+3.5853 (v, millivolts per second, R=0.9949). This indicates that the modified electrode reaction of *p*-AP is a diffusion-controlled process. Figure 5c displayed the relationship between the peak potential (E_p) and the logarithm value of scan rate (log v). With increasing the scan rate, the oxidation peak potential shifted positively and the reduction peak potential shifted negatively. When v> 0.3 Vs^{-1}, the E_{pa} and E_{pc} were linearly dependent on the log v

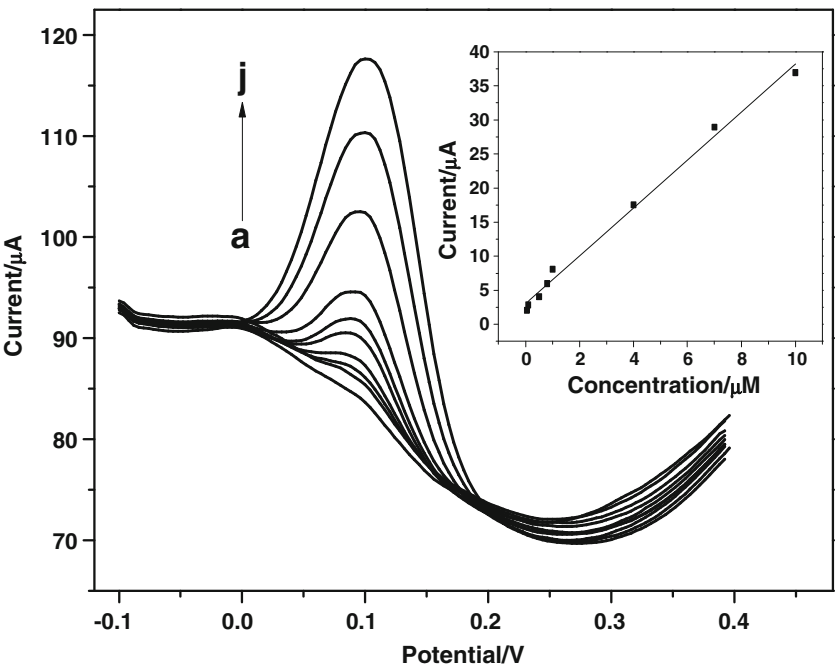

Fig. 7 DPVs on ERGO/GCE for different *p*-AP concentrations (*a–j*): 0, 0.01, 0.05, 0.1, 0.5, 0.8, 1.0, 4.0, 7.0, and 10 μM in 0.1 M PBS. *Inset* is the relationship of current responses to *p*-AP concentration

with the regression equations of E_{pa} (volts)=0.1937+0.0636 log v (v, volts per second), E_{pc} (volts)=0.0584−0.0862 log v (v, volts per second) with R=0.9984 and 0.9946, respectively. Based on the Laviron theory with slopes of the lines $RT/(1-\alpha)nF$ and $-(RT/\alpha nF)$, the value of the electron transfer coefficient (α) and the electron transfer number (n) were calculated as 0.43 and 2.

Effect of pH value

It is generally reported that proton transfer was always involved in the electrochemical oxidation of phenol compounds to form quinone [36, 37]. Therefore, the solution pH will influence the electrochemical behavior of *p*-AP. Figure 6 shows the influence of pH on the redox reaction of *p*-AP at the ERGO-modified electrode. As can be seen, with increasing the solution pH value from 4.49 to 8.04, the redox peak potentials shifted negatively, and the linear regression equations were expressed as E_{pa} (volts)=0.5872−0.0664 pH and E_{pc} (volts)=0.4864−0.0584 pH with correlation coefficients of 0.9953 and 0.9989, respectively. Based on the equation of dEp/dpH=0.059m/n, in which, m is the number of proton, and n is the number of electron transfer, m/n was calculated to be 1.12 and 0.99 for the oxidation and reduction process, respectively. It indicates that the number of proton and electron involved is equal in the electrochemical redox process of *p*-AP. Integrating the results obtained in scan rate and pH studies, two protons and two electrons should be involved in the electrochemical oxidation of *p*-AP to form quinone. In this experiment, the redox peak currents of *p*-AP reached a maximum at a pH value of 6.47; thus, pH 6.47 PBS was chosen as the supporting electrolyte.

Calibration curve

In order to validate the practicality of this method for *p*-AP quantitative analysis, the dependence of the oxidation peak current of *p*-AP on its concentration was investigated in 0.1 M PBS using DPV due to its high sensitivity and excellent resolution (Fig. 7). Under the optimized experimental conditions, the I_{pa} was linearly proportional to the *p*-AP concentration in the range of 0.01–10 μM (inset of Fig. 7). The linear regression equation was I_{pa} (microamps)= 2.983+3.52 c (micromolars), with the correlation coefficient of 0.9964. The detection limit was 2.9×10^{-9} mol L^{-1} based on the signal-to-noise ratio of 3, which is much lower than those obtained on CFME modified with p[NVCzVBSA1] composite (1.0 μM) [8], GCE modified with CRGO (0.057 μM) [35] and SWNTs/POAPE (0.06 μM) [7]. Therefore, the present method based on ERGO/GCE has a much higher sensitivity compared with the above electrochemical methods.

Table 1 Interference of external matters to response of the electrode to 4 μM *p*-AP

Interference	Concentration (μM)	Signal change (%)
$MgSO_4$	4,000	−2.7
$Ca(NO_3)_2$	4,000	−3.6
$ZnSO_4$	4,000	+3.3
$FeSO_4$	4,000	+4.6
$Pb(Ac)_2$	4,000	+2.9
$AlCl_3$	4,000	−4.1
Phenol	200	+4.6
Resorcinol	200	−3.5
Paracetamol	200	−3.8
Glucose	200	−2.9
Dopamine	200	−4.9
Lysine	200	+2.4
o-AP	8	−4.5

Reproducibility and stability are the two vital characteristics for the modified electrode, which should be investigated for analytical determination [38]. The measurement reproducibility of the ERGO-modified electrode was studied with the same 4-AP concentration. After each measurement, the surface of ERGO-modified electrode undergoes ten successive CV sweeps between −0.2 and 0.6 V at 100 mV s^{-1} in the 0.1 M PBS (pH 6.47) to be regenerated. Determination of 4 μM 4-AP using six electrodes prepared independently with the same procedure results in a relative standard deviation (RSD) of 4.6 %. One modified electrode for eight times repetitive measurements of the oxidation currents of 4-AP results in a RSD of only 2.5 %. These results indicate a good reproducibility of ERGO-modified electrode. And the response of the modified electrode to 4.0 μM 4-AP only decreased 12.6 % of its initial response after stored in a refrigerator at 4 °C for a month. This result revealed that the present modified electrode has excellent stability for the detection of *p*-AP.

Interferences

The influence of potential coexistent interference compounds has been studied for the possible analytical application of the proposed method. If the presence of some metal ions or

Table 2 Determination of *p*-AP in water samples (n=4)

	Tap water *p*-AP	River water *p*-AP	Wastewater *p*-AP
Added (μM)	3.00	3.00	3.00
Determined (μM)	2.92	2.92	3.05
RSD (%)	2.3	4.6	3.8
Recovery (%)	97.3	98.7	101.7

organic compounds altered the average current signal of *p*-AP by less than ±5 %, we considered that caused no interference. In the case of 4 μM *p*-AP, the influences of several inorganic and organic species on the *p*-AP signals were tested, and the results were shown in Table 1. One thousand-fold of Mg^{2+}, Ca^{2+}, Zn^{2+}, Fe^{2+}, Pb^{2+}, Al^{3+}, Cl^-, NO_3^-, SO_4^{2-}, 50-fold of phenol, resorcinol, paracetamol, glucose, dopamine, lysine, and twofold of *o*-AP did not interfere with the oxidation signal of 4 μM *p*-AP. The results clearly proved the reasonable selectivity of the proposed method for the oxidation of *p*-AP.

Analysis of real water samples

In order to assess the applications of the developed method for sensitive determination of *p*-AP, synthetic water samples containing *p*-AP in local tap water, river water, and wastewater without any pretreatment were tested. The standard addition method was used to determine *p*-AP in water samples. All the samples were determined for four times under the same conditions. The results are listed in Table 2. The recoveries of *p*-AP at ERGO/GCE are in the range from 97.3 to 101.7 %, declaring that this method is effective and reliable.

Conclusions

In this article, we have successfully employed an electrochemical reduction method using GO as a precursor for the fabrication of ERGO-modified GCE. The modified electrode for the determination of *p*-AP was demonstrated. This modified electrode showed an excellent electrocatalytic activity towards the redox reaction of *p*-AP. Owing to the unique properties of ERGO, including extraordinary electronic transport characteristics, high surface area, and good π–π interaction, the ERGO-modified electrode obviously promotes the sensitivity of the determination of *p*-AP with a low detection limit. The proposed method was applied to detect *p*-AP in water samples with satisfactory recoveries from 97.3 to 101.7 %.

Acknowledgments We would like to acknowledge the financial support from the National Natural Science Foundation of China (No. 21105002), Anyang Technology Research Program (No 208), and the Innovative Foundation for the college students of Anyang Normal University (ASCX/2011-Z12).

References

1. Yesilada A, Erdogan H, Ertan M (1991) Anal Lett 24:129–138
2. The European Pharmacopeial Convention (2007) The Sixth Edition European Pharmacopoeia, pp.49
3. Chen X, Parker SG, Zou G, Su W, Zhang Q (2010) ACS Nano 4:6387–6394
4. Monser L, Darghouth F (2002) J Pharm Biomed Anal 27:851–860
5. Pumera M, Llopis X, Merkoci A, Alegret S (2006) Microchim Acta 152:261–265
6. Mohamed F, AbdAllah M, Shammat S (1997) Talanta 44:61–68
7. Wang Z, Zhu H, Zhang H, Gao G, Sun Z, Liu H, Zhao X (2009) Electrochimi Acta 54:7531–7535
8. Jamal M, Sarac AS, Magner E (2004) Sensor Actuat B-Chem 97:59–66
9. Novoselov KS, Geim AK, Morozov SV, Jiang D, Zhang Y, Dubonos SV, Grigorieva IV, Firsov AA (2004) Science 306:666–669
10. Huang X, Qi X, Boey F, Zhang H (2012) Chem Soc Rev 41:666–686
11. Huang X, Yin Z, Wu S, Qi X, He Q, Zhang Q, Yan Q, Boey F, Zhang H (2011) Small 7:1876–1902
12. Shao Y, Wang J, Wu H, Liu J, Aksay IA, Lin Y (2010) Electroanalysis 22:1027–1036
13. Chen D, Tang L, Li J (2010) Chem Soc Rev 39:3157–3180
14. Shang NG, Papakonstantinou P, McMullan M, Chu M, Stamboulis A, Potenza A, Dhesi SS, Marchetto H (2008) Adv Funct Mater 18:3506–3514
15. Li J, Guo S, Zhai Y, Wang E (2009) Electrochem Commun 11:1085–1088
16. Li J, Guo S, Zhai Y, Wang E (2009) Anal Chim Acta 649:196–201
17. Kang X, Wang J, Wu H, Liu J, Aksay IA, Lin Y (2010) Talanta 81:754–759
18. Stankovich S, Dikin DA, Piner RD, Kohlhaas KA, Kleinhammes A, Jia YY, Wu Y, Nguyen ST, Ruoff RS (2007) Carbon 45:1558–1565
19. Li D, Muller MB, Gilje S, Kaner RB, Wallace GG (2008) Nat Nanotechnol 3:101–105
20. Si Y, Samulski ET (2008) Nano Lett 8:1679–1682
21. Guo HL, Wang XF, Qian QY, Wang FB, Xia XH (2009) ACS Nano 3:2653–2659
22. Wang Z, Zhou X, Zhang J, Boey F, Zhang H (2009) J Phys Chem C 113:14071–14075
23. Zhou M, Wang Y, Zhai Y, Zhai J, Ren W, Wang F, Dong S (2009) Chem Eur J 15:6116–6120
24. Wang Z, Zhang J, Chen P, Zhou X, Yang Y, Wu S, Niu L, Han Y, Wang L, Chen P, Boey F, Zhang Q, Liedberg B, Zhang H (2011) Biosens Bioelectron 26:3881–3886
25. Uhm S, Tuyen NH, Lee J (2011) Electrochem Commun 13:677–680
26. Zhou YG, Chen JJ, Wang FB, Sheng ZH, Xia XH (2010) Chem Commun 46:5951–5953
27. Zhu C, Guo S, Fang Y, Han L, Wang E, Dong S (2011) Nano Res 4:648–657
28. Feng XM, Li RM, Ma YW, Chen RF, Shi NE, Fan QL, Huang W (2011) Adv Funct Mater 21:2989–2996
29. Kovtyukhova NI, Ollivier PJ, Martin BR, Mallouk TE, Chizhik SA, Buzaneva EV, Gorchinskiy AD (1999) Chem Mater 11:771–778
30. Hummers WS, Offeman RE (1958) J Am Chem Soc 80:1339–1339
31. Wu H, Wang J, Kang X, Wang C, Wang D, Liu J, Aksay IA, Lin Y (2009) Talanta 80:403–406
32. Wang C, Zhang L, Guo Z, Xu J, Wang H, Zhai K, Zhuo X (2010) Microchim Acta 169:1–6
33. Wang Y, Li Y, Tang L, Lu J, Li J (2009) Electrochem Commun 11:889–892
34. Zhou M, Zhai Y, Dong S (2009) Anal Chem 81:5603–5613
35. Yin H, Ma Q, Zhou Y, Ai S, Zhu L (2010) Electrochimi Acta 55:7102–7108
36. Wang Z, Li S, Lv Q (2007) Sensor Actuat B-Chem 127:420–425
37. Liu AL, Zhang SB, Chen W, Lin XH, Xia XH (2008) Biosens Bioelectron 23:1488–1495
38. Liu X, Li Y, Liu X, Zeng X, Kong B, Luo S, Wei W (2011) J Solid State. Electrochem. doi:10.1007/s10008-011-1428-2